Bond Between Near-Surface Mounted Carbon-Fiber-Reinforced Polymer Laminate Strips and Concrete

José Manuel de Sena Cruz[1] and Joaquim António Oliveira de Barros[2]

Abstract: In recent years, a strengthening technique based on near-surface mounted (NSM) laminate strips of carbon-fiber-reinforced polymer (CFRP) has been used to increase the load-carrying capacity of concrete and masonry structures by introducing laminate strips into precut grooves on the concrete cover of the elements to be strengthened. The high experimentally derived levels of strength efficacy with concrete columns, beams, and masonry panels have presented NSM as a viable and promising technique. This practice requires no surface preparation work and, after cutting the groove, requires minimal installation time compared to the externally bonded reinforcing technique. A further advantage associated with NSM CFRP is its ability to significantly reduce the probability of harm resulting from fire, acts of vandalism, mechanical damage, and aging effects. To assess the bond behavior of CFRP to concrete, pullout-bending tests have been carried out. The influences of bond length and concrete strength on bond behavior are analyzed, the tests are described, and the results are presented and discussed in detail. Finally, a local stress-slip relationship is determined based on both experimental results and a numerical strategy.

DOI: 10.1061/(ASCE)1090-0268(2004)8:6(519)

CE Database subject headings: Bonding; Bonding strength; Fiber reinforced polymers; Concrete; Laminates.

Introduction

During the last decade, conventional materials such as steel and concrete have been replaced by fiber-reinforced polymer (FRP) materials for the strengthening of concrete structures (CEB-FIB 2001; ACI 2002). The most current strengthening technique is based on applying the FRP onto the faces of the elements to be strengthened and is designated the externally bonded reinforcing (EBR) technique. Research to date has revealed that this technique cannot mobilize the full tensile strength of FRP materials because of premature debonding (Mukhopadhyaya and Swamy 2001; Nguyen et al. 2001). The reinforcing performance of FRP materials can be negatively affected by the effect of freeze/thaw cycles (Toutanji and Balaguru 1998) and decreases significantly when submitted to high and low temperatures (Pantuso et al. 2000). Furthermore, EBR systems are susceptible to damage caused by vandalism and mechanical malfunctions.

Several attempts have been made to overcome the aforementioned drawbacks. The most promising of these has been the use of near-surface mounted (NSM) FRP rods by installing glass or carbon FRP rods in precut grooves on the concrete cover of the elements to be strengthened (De Lorenzis et al. 2000). This technique has been used in some applications and several benefits have been pointed out (Warren 1998; Alkhrdaji et al. 1999; Hogue et al. 1999; Tumialan et al. 1999; Warren 2000; Emmons et al. 2001). The bond performance of this technique has been extensively analyzed in recent years (De Lorenzis 2002).

Other researchers have proposed similar strengthening techniques but, instead of rods, have used laminate strips of CFRP (Blaschko and Zilch 1999; Ferreira 2000). The benefits in terms of load-carrying capacity and ductility showed that this technique is promising for strengthening not only concrete elements failing in bending (Ferreira 2000; Barros and Fortes 2002), but also reinforced concrete beams failing in shear (Barros and Dias 2003).

Since bond behavior analysis is a requirement for understanding the stress transfer process between concrete and CFRP, the present work conducts a pullout-bending test similar to the one proposed by RILEM (1982) for assessing the bond characteristics of conventional steel rods. Using the same groove size and epoxy adhesive, bond behavior is analyzed to determine the influences of both bond length and concrete strength.

Using a method similar to the one proposed by Focacci et al. (2000) and taking into account the results obtained from the carried-out experiments, a local bond stress-slip relationship, $\tau-s$, is defined. The present work describes the carried-out tests and presents and analyzes the most significant results obtained. The numerical strategy implemented for the evaluation of the $\tau-s$ law is also described.

Experimental Program

Specimen and Test Configuration

The pullout-bending test is schematically represented in Fig. 1. The specimen is composed of two blocks: block B, where the CFRP is fixed to concrete along a bonded length of 325 mm, and block A, where the CFRP is bonded to concrete using distinct bond lengths (test region). This configuration assures that the bond failure will occur in block A.

[1]PhD Student, Dept. of Civil Engineering, Univ. of Minho, Azurém, 4810-058 Guimarães, Portugal.

[2]Assistant Professor, Dept. of Civil Engineering, Univ. of Minho, Azurém, 4810-058 Guimarães, Portugal.

Note. Discussion open until May 1, 2005. Separate discussions must be submitted for individual papers. To extend the closing date by one month, a written request must be filed with the ASCE Managing Editor. The manuscript for this paper was submitted for review and possible publication on April 30, 2003; approved on January 26, 2004. This paper is part of the *Journal of Composites for Construction*, Vol. 8, No. 6, December 1, 2004. ©ASCE, ISSN 1090-0268/2004/6-519–527/$18.00.

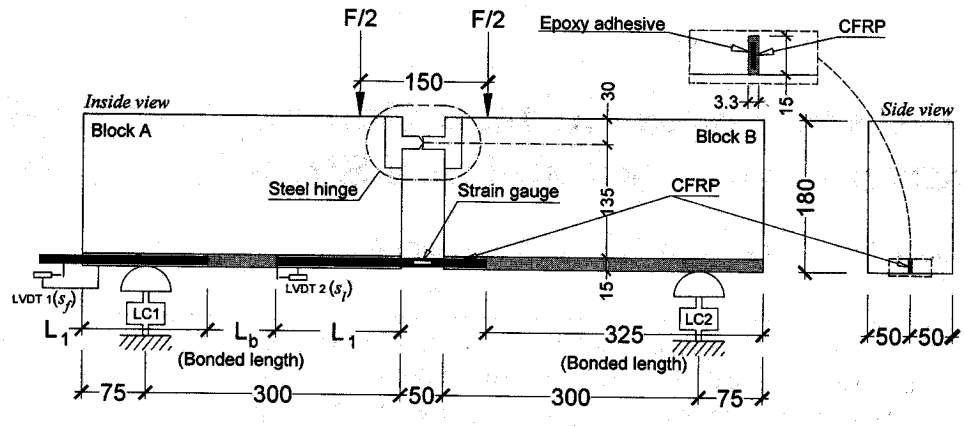

Fig. 1. Specimen of pullout-bending test

The groove where the CFRP is inserted has a 15-mm depth and a 3.3-mm width (Fig. 1). The displacement transducer LVDT2 was used to control the test at 5 μm/s and to measure the slip at the loaded end, s_l, while LVDT1 records the slip at the free end, s_f. The strain gauge glued to the CFRP at the symmetry axis of the specimen is used to estimate the pullout force on the CFRP at the loaded end. The applied forces are measured using two load cells (LC1 and LC2) placed at the supports of the specimen. The characteristics of the displacement transducers, strain gauge, and load cells are described elsewhere (Sena-Cruz and Barros 2002b).

Test Procedure

According to the recommendations proposed in research evaluating the bond length of FRP on EBR technique (German 1997; Rostasy 1998; Concrete 2000), and taking into account data obtained from tests carried out with utilized materials, a value of 95 mm is estimated for the upper bound of the bond length (Sena-Cruz and Barros 2002a,b). To avoid rupture of the CFRP on the pullout-bending test, a maximum bond length of 80 mm is selected. Bond lengths of 40, 60, and 80 mm are considered for assessing its influence on bond behavior.

Table 1. Mix Compositions and Average Compression Strength of Concrete of Series Tested

Designation of series	Composition (kg/m³)[a]					f_{cm}[b] (MPa)
	FS	CS	CA	C	W	
fcm35_Lb40	—	745	943	350	210	34.5 (6.94%)
fcm35_Lb60	—	745	943	350	210	33.0 (4.24%)
fcm35_Lb80	—	745	943	350	210	37.2 (1.50%)
fcm45_Lb40	—	627	1,049	400	200	46.2 (0.53%)
fcm45_Lb60	—	627	1,049	400	200	41.4 (2.32%)
fcm45_Lb80	—	627	1,049	400	200	47.1 (1.65%)
fcm70_Lb40	427	419	848	500	150	69.9 (0.87%)
fcm70_Lb60	427	419	848	500	150	70.3 (8.24%)
fcm70_Lb80	427	419	848	500	150	69.2 (7.47%)

[a]FS=fine sand (0–3 mm); CS=coarse sand (0–5 mm); CA=coarse aggregates (5–15 mm); C=Cement Secil 42.5 type I; W=water; in series fcm70 it was applied 7.8 L/m³ of Rheobuild 1000 superplasticized.

[b]Values in parentheses are coefficients of variation of corresponding series.

Having assumed that, in the majority of concrete structures needing strengthening intervention, the concrete compression strengths range from 30 to 50 MPa, two concrete mixes are designed with the average compression strength near the limits of this range (35 and 45 MPa). To appraise the influence of concrete quality on CFRP bond behavior, a third composition of high-strength concrete (70 MPa) has also been designed. The experimental program therefore consists of nine series, each composed of three specimens. A generic series has the designation of fcmXX_LbYY, where XX represents the concrete compression strength class, in megapascals, and YY the CFRP bond length, in millimeters.

Specimen Preparation

After a period of 28 days, specimens are removed from the curing room water tank to make the grooves where the CFRP is to be inserted. Each groove is made on a sawcut table machine. To assure proper concrete drying before bonding the CFRP to the concrete, specimens remain in the natural laboratory environment for eight consecutive days. Prior to CFRP installation, both the groove and the CFRP are prepped. The former is cleaned by compressed air and the latter by acetone. In the regions where the CFRP is to be bonded to concrete, the groove is filled with an epoxy adhesive and the lateral faces of the CFRP are covered by a thin layer of the epoxy adhesive prepared according to supplier recommendations. Then the CFRP is inserted into the groove and

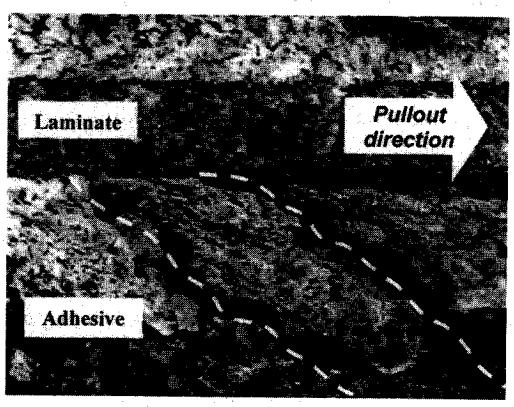

Fig. 2. Mechanism of adhesive failure

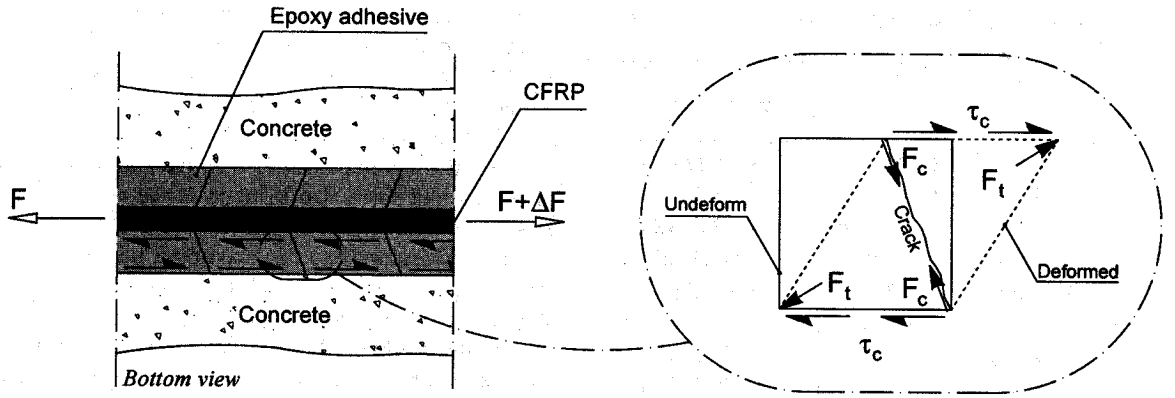

Fig. 3. Micromechanisms justifying crack pattern developed on epoxy adhesive

is slightly pressed to force the epoxy adhesive to flow between the CFRP and the groove sides. Finally, the excess epoxy is removed and the surface is leveled.

Material Properties

Concrete compositions are included in Table 1, and further details related to concrete manufacturing are described elsewhere (Sena-Cruz and Barros 2002b). To avoid the failure of the specimen in shear, 60 kg/m^3 of hooked end steel fibers are added to the concrete composition (Sena-Cruz et al. 2001). For this content of fibers, only the concrete postcracking tensile residual strength is significantly affected by fiber reinforcement mechanisms (Rossi 1998; Barros and Figueiras 1999). Since concrete cracking is not expected to occur in the bonding zone, the influence of adding fibers to concrete is marginal for bond behavior (Ezeldin and Balaguru 1989).

The concrete compression strength is obtained from tests with cylinder specimens (150-mm in diameter and 300 mm high). The concrete average compression strength of fibrous cement mortar (fcm) results from tests carried out on more than three specimens at the age of the pullout-bending tests (Table 1).

From 20 measures it has been verified that the CFRP cross section has a thickness of 1.39 mm and a width of 9.34 mm. From three uniaxial tensile tests carried out according to the recommendations of ISO (1997), a Young's modulus of 158.3±2.6 GPa, a tensile strength of 2,739.5±85.7 MPa, and an ultimate tensile strain of 1.7±0.04% have been obtained.

To assess the compression and bending strengths of the epoxy adhesive used for bonding the CFRP to concrete, three point bending tests and compression tests have been carried out according to the recommendations of CEN (1987). As a result, a bending tensile strength of 25.8±2.1 MPa and a compression strength of 44.4±5.3 MPa have been obtained.

Results

Failure Modes

The photo of the laminate-adhesive-concrete bonding zone in Fig. 2 is obtained from an optical microscope and reveals that the failure occurs in the concrete-adhesive and adhesive-laminate interfaces. A fish spine crack pattern can be observed on the epoxy adhesive, which is explainable in terms of the deformations im-

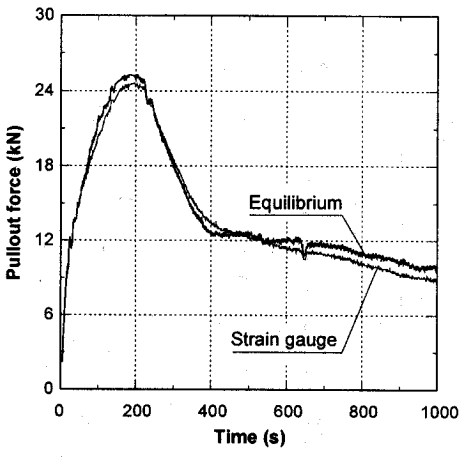

Fig. 4. Time evolution of pullout force in carbon-fiber-reinforced polymer of specimen B3_fcm45_Lb80 from two approaches

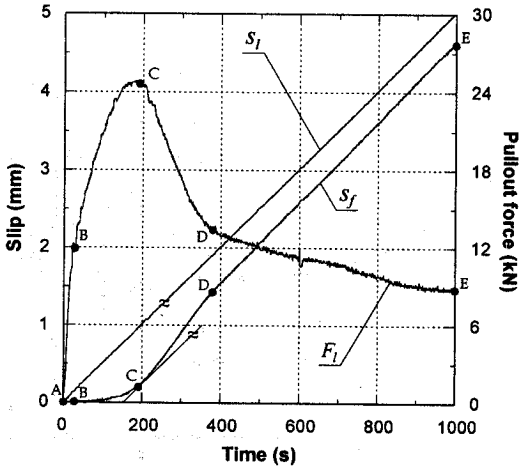

Fig. 5. Time evolution of pullout force (F_l) and slip at free end (s_f) and loaded end (s_l)

Table 2. Average Values of $F_l/F_{l\,max}$ Ratio for Points B, C, and D (Fig. 5)

Series	Ratio $F_l/F_{l\,max}$		
	B	C	D
fcm35_Lb40	0.563 (30.0%)	0.978 (0.7%)	0.805 (2.9%)
fcm35_Lb60	0.817 (6.0%)	0.991 (1.0%)	0.601 (9.3%)
fcm35_Lb80	0.767 (5.3%)	0.987 (1.4%)	0.663 (6.4%)
fcm45_Lb40	0.662 (12.0%)	0.996 (0.7%)	0.798 (11.2%)
fcm45_Lb60	0.654 (24.3%)	0.987 (1.0%)	0.661 (7.0%)
fcm45_Lb80	0.657 (23.3%)	0.942 (9.0%)	0.584 (7.0%)
fcm70_Lb40	0.677 (9.0%)	0.971 (0.9%)	0.730 (7.4%)
fcm70_Lb60	0.705 (18.8%)	0.981 (2.0%)	0.759 (2.2%)
fcm70_Lb80	0.669 (31.9%)	0.990 (0.9%)	0.708 (5.8%)

Note: Values in parentheses are coefficients of variation of corresponding series.

posed by the CFRP during pulling out, as schematically represented in Fig. 3. The average angle between the crack surface and the CFRP direction is 33°. Cracks on the concrete surface have never been observed, justifying the previous hypothesis that concrete tensile strength is not a mandatory property in this specific bond test.

Pullout Force

To evaluate the pullout force on the CFRP (at the loaded end of the bond length), F_l, two approaches have been adopted. The first uses the force values measured on the load cells and takes into account the internal arm, that is, the distance between the CFRP and the contact of the two parts of the steel hinge (Fig. 1). The second uses the strain values recorded by the strain gauge glued on the CFRP and takes into account the values of 160 GPa and 12.98 mm^2 for the Young's modulus and the cross-sectional area of the CFRP, respectively. Although these two approaches lead to similar results (Fig. 4), the second has been selected in this work.

Slip at Free and Loaded Ends

Fig. 5 depicts a typical time evolution of the pullout force and the slips measured at the free (LVDT1) and loaded (LVDT2) ends (Fig. 1). Analyzing the time evolution of the slips, the following four branches can be distinguished:

- AB where slip occurs only at the loaded end;
- BC where slips at loaded and free ends occur and the slip rate at the loaded end is the largest;
- CD where the slip rate at the free end is larger than the slip rate at the loaded end; and
- DE where slip rates are similar at both free and loaded ends.

Point B roughly coincides with the end of the linear evolution of the pullout force. Up to point B the slip is governed by the elastic deformation of the CFRP and epoxy adhesive materials. Point C corresponds to the maximum pullout force. During the stage corresponding to branch BC, both the pullout force and the slip at the free end have a nonlinear evolution. This can be justified by the nonlinear behavior of the epoxy adhesive as well as the debonding process at laminate-adhesive and concrete-adhesive interfaces. Point D is located at the border of two branches of a very distinct slope. Due to the degradation of the bonding mechanisms at laminate-adhesive-concrete interfaces as well as to adhesive cracking, a significant decay of the pullout force can be observed from point C to point D. Due to this decrease, an elastic strain release on the CFRP occurs, thereby justifying the fact that the slip rate at the free end is larger than the slip rate at the loaded end. After point D, the pullout resistance is mainly due to friction mechanisms at both the laminate-adhesive and concrete-adhesive interfaces, resulting in a quasi-rigid body movement of the CFRP at the bonded zone, with similar slip rates at both free and loaded ends.

The values of the $F_l/F_{l\,max}$ ratio for the points B, C, and D are evaluated from the obtained experimental results where F_l is the force at B, C, or D points and $F_{l\,max}$ is the maximum registered pullout force. These results are included in Table 2, from which it can be verified that the force at point C is near the $F_{l\,max}$ value; the forces at points B and D are about 70% of the $F_{l\,max}$ value but with a large scatter; and concrete strength has a marginal influence on the $F_l/F_{l\,max}$ values for these points. Homogeneity of thickness and of physical properties of the epoxy adhesive along the bond length are difficult to assure. Consequently, some nonlinear deformations of the epoxy adhesive may have occurred during the stage corresponding to branch AB, especially at the loaded end, thereby contributing to the scatter of $F_l/F_{l\,max}$ obtained at point B. It has been verified that the rigidity and the strength of the epoxy adhesive are dependent on the presence of inevitable voids (Sena-Cruz et al. 2001). Since the variability of these epoxy properties influences the stress transfer between the laminate and the concrete, it may also have contributed to the scatter of $F_l/F_{l\,max}$ at point C.

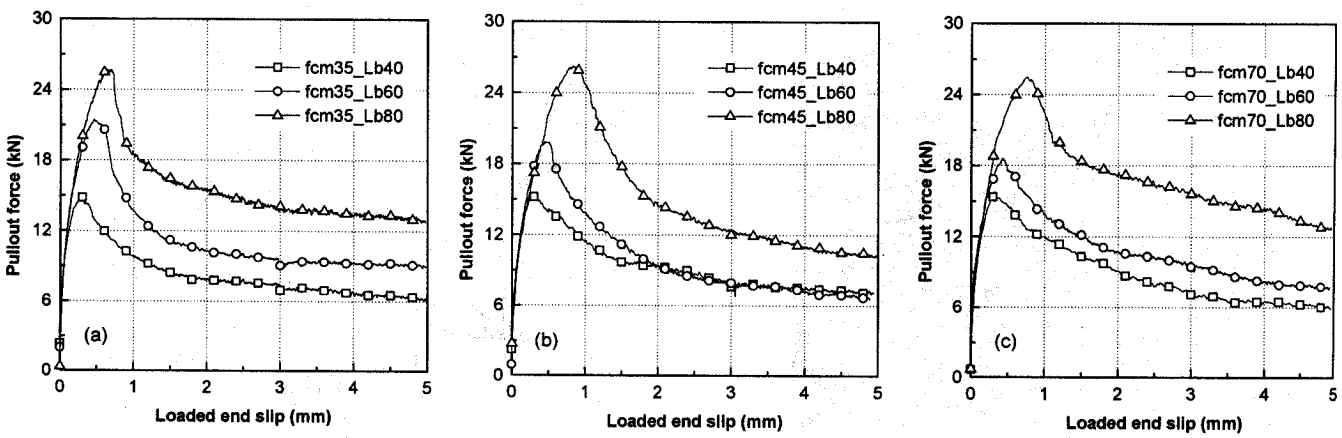

Fig. 6. Pullout force-loaded end slip relationship for series of (a) 35 MPa, (b) 45 MPa and (c) 70 MPa concrete compression strength classes

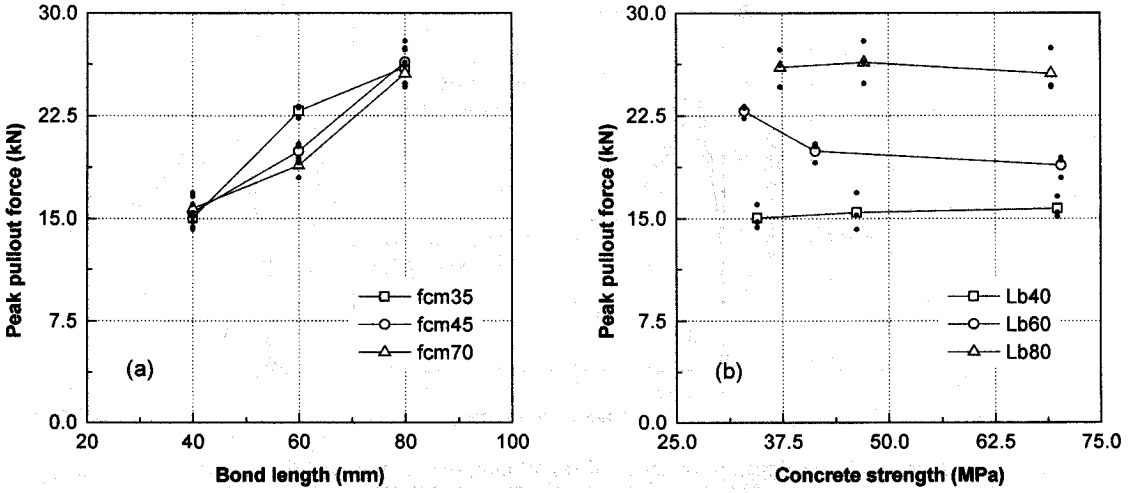

Fig. 7. Influence of (a) bond length and (b) concrete strength on peak pullout force

Pullout Force versus Slip

Fig. 6 depicts the relationship between the pullout force and the slip at the loaded end for the series of distinct concrete strength classes. Each curve is the average response of three specimens. As is expected, the pullout force is increased with the bond length, L_b, [see Fig. 7(a), where the influence of the L_b on the peak pullout force is represented]. Since epoxy adhesive has remarkably nonlinear behavior (Sena-Cruz et al. 2001) and its volume increases with L_b, the nonlinear branch before peak pullout force also increases with L_b. As Fig. 7(b) and the results in Table 3 reveal, the influence of the concrete strength is marginal, especially in the $F_{l\,\max}$.

Bond Stress versus Slip

Bond stress is obtained through dividing the pullout force by the contact area between CFRP and epoxy adhesive, $F_l/(2(w_f+t_f)L_b)$ where F_l is the pullout force and w_f and t_f are the width and thickness of the CFRP. Fig. 8 illustrates the relationship between the bond stress and the slip at the loaded end for the series of distinct bond lengths. Peak bond stress, τ_{max}, decreases with bond length and is practically insensitive to concrete strength (see also Fig. 9 and Table 3).

Table 3. Average Values of Main Parameters Evaluated

Series	$F_{l\,\max}$ (kN)	τ_{max} (MPa)	$\sigma_{l\,\max}/f_{fu}$ (%)	$s_{l\,\max}$ (mm)
fcm35_Lb40	15.0 (5.8%)	17.5	42.1	0.29 (21.5%)
fcm45_Lb40	15.5 (2.0%)	18.1	43.5	0.27 (26.8%)
fcm70_Lb40	15.7 (8.8%)	18.3	44.0	0.32 (10.5%)
fcm35_Lb60	22.8 (8.7%)	17.7	64.0	0.49 (5.8%)
fcm45_Lb60	19.9 (3.7%)	15.5	55.8	0.46 (8.8%)
fcm70_Lb60	18.9 (5.8%)	14.7	52.9	0.40 (10.0%)
fcm35_Lb80	22.4 (5.0%)	13.0	62.1	0.65 (16.0%)
fcm45Lb80	26.4 (4.2%)	15.4	73.9	0.84 (30.6%)
fcm70_Lb80	25.6 (6.2%)	14.9	71.6	0.74 (3.0%)

Note: Values in parentheses are coefficients of variation of corresponding series.

Carbon-Fiber-Reinforced Polymer Stress at Peak Pullout Force

The influences of bond length and concrete strength on the stress of CFRP at peak pullout force, $\sigma_{l\,\max}$, are represented in Figs. 10(a and b), respectively, where $\sigma_{l\,\max}$ is normalized by the CFRP tensile strength, f_{fu}=2,740 MPa. This influence can also be assessed from the results included in Table 3. Fig. 10 reveals that in general $\sigma_{l\,\max}/f_{fu}$ increases with the bond length and is independent of the concrete strength.

Loaded End Slip at Peak Pullout Force

The influences of bond length and concrete strength on the loaded end slip at peak pullout force, $s_{l\,\max}$, are represented in Figs. 11(a and b), respectively. A linear increasing trend of $s_{l\,\max}$ with the bond length is observed in Fig. 11(a), while an independence of the $s_{l\,\max}$ on the concrete strength is shown in Fig. 11(b) (Table 3).

Local Bond Stress-Slip Relationship

The slip of CFRP bonded into concrete is governed by the following differential equation (Sena-Cruz and Barros 2003):

$$\frac{d^2s}{dx^2} = \frac{2}{t_f E_f}\tau(s) \tag{1}$$

where E_f is the Young's modulus of the CFRP and $\tau(s)$ is the bond stress acting on the contact surface between CFRP and epoxy adhesive in the length of dx.

Based on the methodology used for the bonding of steel bars to concrete, several approaches have been developed to establish a local bond stress-slip relationship, $\tau-s$, for FRP rods (Larralde and Silva-Rodriguez 1993; Malvar 1995; Cosenza et al. 1997; Focacci et al. 2000; De Lorenzis et al. 2002). The method proposed by Focacci et al. (2000) is used in the present work, with necessary adjustments to account for the specificities of the present strengthening technique. The local bond stress-slip relationship consists of the following two equations:

$$\tau(s) = \tau_m \times \left(\frac{s}{s_m}\right)^{\alpha}, \quad \text{if } s \leq s_m \tag{2}$$

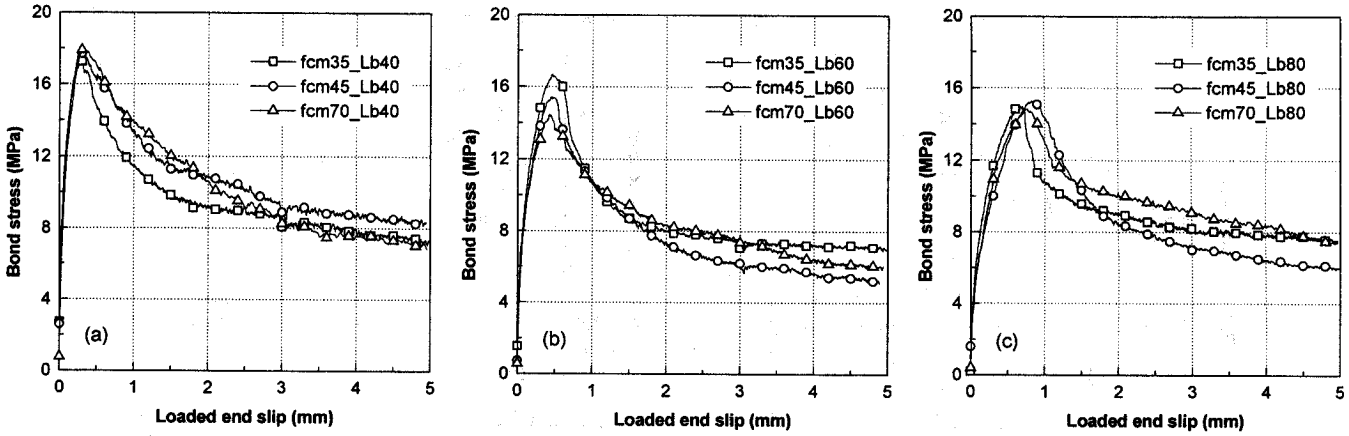

Fig. 8. Bond stress-slip relationship for series of (a) 40 mm, (b) 60 mm, and (c) 80 mm bond lengths

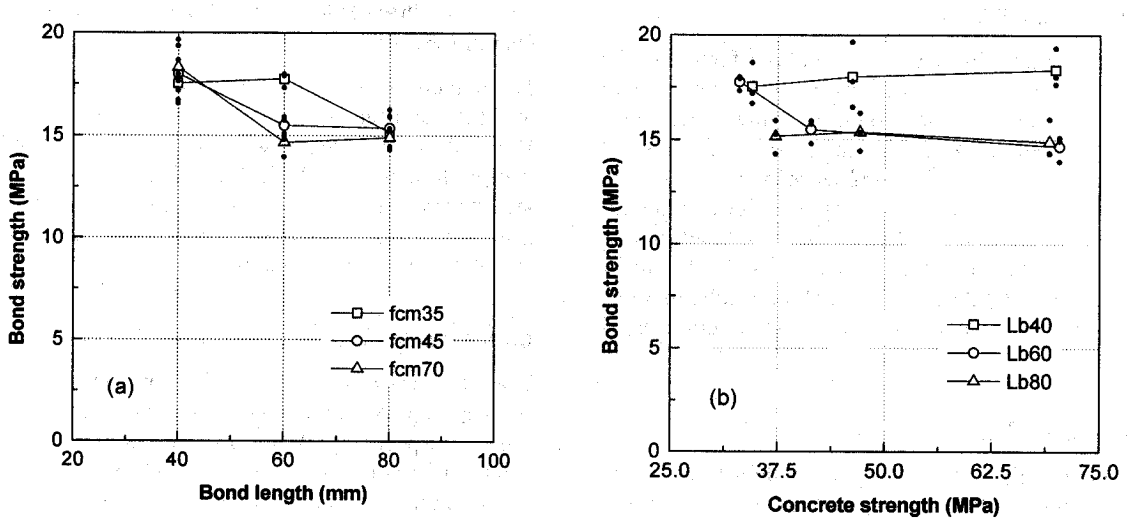

Fig. 9. Influences of (a) bond length and (b) concrete strength on bond strength

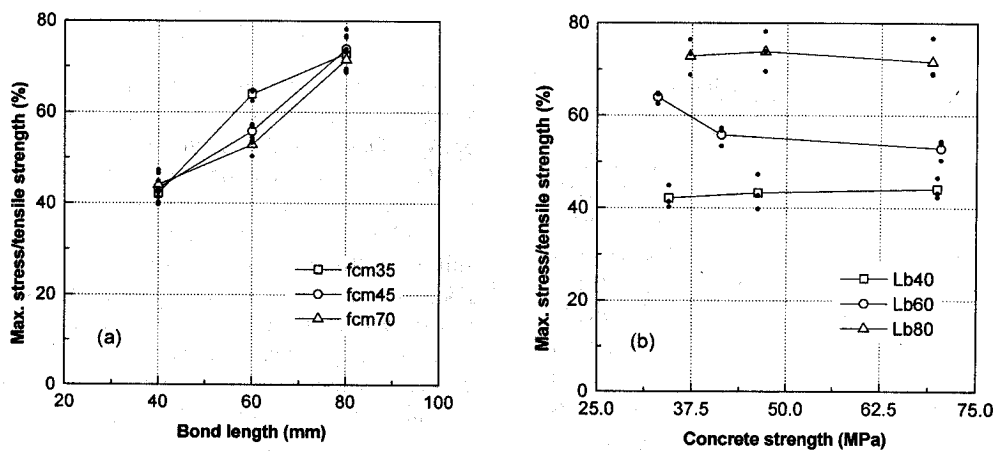

Fig. 10. Influences of (a) bond length and (b) concrete strength on tensile ratio $\sigma_{l\,\max}/f_{fu}$

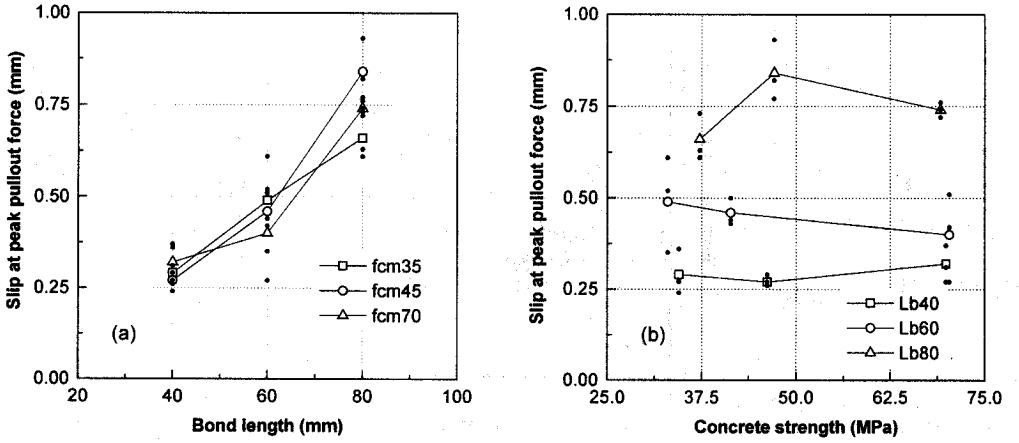

Fig. 11. Influences of (a) bond length and (b) concrete strength on loaded end slip at peak pullout force

$$\tau(s) = \tau_m \times \left(\frac{s}{s_m}\right)^{-\alpha'}, \quad \text{if } s > s_m \tag{3}$$

where τ_m and s_m are the bond strength and its corresponding slip, and α and α' are parameters defining the shape of the curves. This law has been selected for its simplicity and ability to simulate the phenomena under discussion.

Using the slip at the free end, the slip at the loaded end, and the pullout force values obtained from the pullout bending tests, a numerical strategy described elsewhere (Sena-Cruz and Barros 2003) has been developed in order to determine the parameter values s_m, τ_m, α, and α' of Eqs. (2) and (3) that fit, as much as possible, the differential Eq. (1) that governs the slip of the CFRP bonded to concrete.

The performance of the developed method is well demonstrated in Fig. 12, where the experimental and the numerical slip-pullout force relationships are compared for the specimen B2 of the fcm45_Lb80 series. A similar performance has been observed in the remaining series. At the peak pullout force, the evolution of the slip, bond stress and axial force along the bond length are shown in Fig. 13. At this load level the bond behavior is essentially nonlinear and half of the bond length is in the softening phase.

Fig. 14 shows that the loaded end slip *versus* pullout force relationship, derived analytically, fits well within the corresponding experimental envelope. An analogous performance has been obtained in the remaining series.

The value parameters of this law and the error obtained in each analysis are included in Table 4. The error is the difference, in absolute value, between the areas corresponding to the experimental and analytical curves divided by the area of the experimental curve. From these data the following observations can be pointed out:

- The margin of error in each series is quite acceptable;
- A reasonable coefficient of variation is obtained in the average bond strength;
- A large scatter in the values of s_m, α, and α' is obtained; and
- Since the deformability of the epoxy adhesive is neglected in the approach developed (Sena-Cruz and Barros 2003), s_m increases with the bond length.

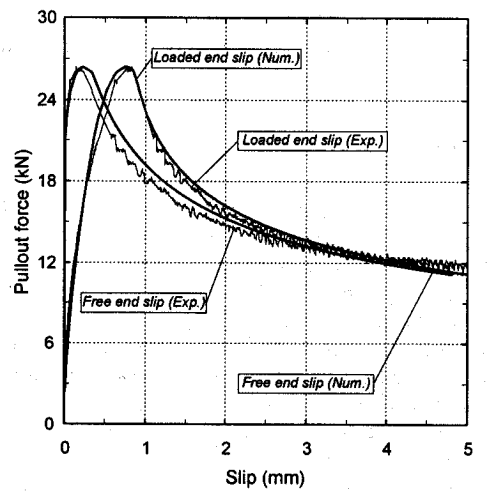

Fig. 12. Simulation of specimen B2_fcm45_Lb80

Conclusions

Pullout-bending tests were carried out to assess the bond performance of laminate strips of carbon-fiber-reinforced polymer (CFRP) to concrete. The influences of the bond length (L_b) and the concrete strength (fcm) were analyzed, testing series with L_b=40, 60, and 80 mm, and fcm=35, 45, and 70 MPa. A physical interpretation of the evolution of the pullout force and the slip at free and loaded ends was given based on the involved micromechanisms. From the results obtained in the experimental program, the following conclusions can be pointed out:

- The nonlinear branch before peak pullout force increased with L_b;

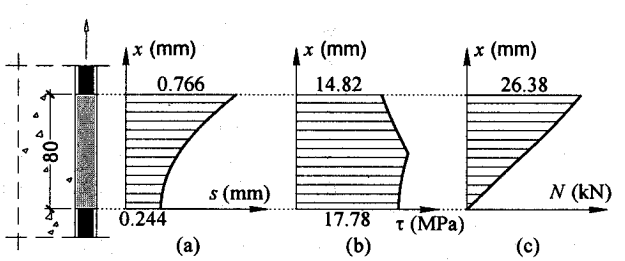

Fig. 13. Evolution of (a) slip, (b) bond stress, and (c) axial force along bond length of specimen B2_fcm45_Lb80

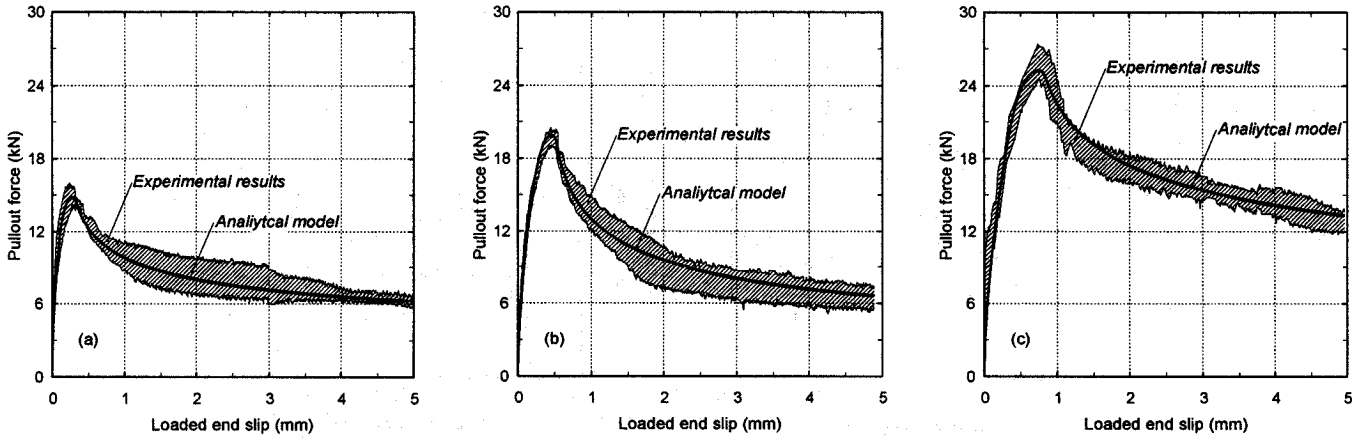

Fig. 14. Analytical and experimental results of (a) series fcm35_Lb40, (b) fcm45_Lb60, and (c) fcm70_Lb80

- The peak pullout force increased with L_b;
- The influence of the concrete strength on the pullout behavior was marginal;
- The bond strength ranged from 13 to 18 MPa, revealed a tendency to decrease with the increase of L_b, and was practically insensitive to concrete strength;
- The ratio between the maximum tensile stress recorded on CFRP and its tensile strength increased with L_b and was independent of concrete strength; and
- The loaded end slip at peak pullout force revealed a linear increasing trend with L_b and an independence of concrete strength.

Using the data obtained in experimental tests and developing a numerical strategy to solve the second-order differential equation that governs the slip phenomenon, the values of the parameters that define a local bond stress-slip relationship, τ–s, were obtained. Since the deformability of the epoxy adhesive was not measured, the resulting τ–s relationship was dependent on the slip at peak bond stress.

Acknowledgments

The writers of the present work wish to acknowledge support provided by the S&P, Bettor MBT Portugal, Secil, and Solusel companies and the colaboration of the Cemacom. The second writer wishes to acknowledge the grant SFRH/BSAB/291/2002 provided by FCT and FSE.

Table 4. Values of Parameters Defining Local Bond Stress-Slip Relationship

Series	s_m (mm)	τ_m (MPa)	α	α'	Error (%)
fcm35_Lb40	0.180	20.60	0.13	−0.27	2.04
fcm35_Lb60	0.228	20.68	0.19	−0.35	5.92
fcm35_Lb80	0.290	18.90	0.17	−0.33	6.96
fcm45_Lb40	0.144	21.40	0.21	−0.23	4.66
fcm45_Lb60	0.231	19.50	0.24	−0.39	2.98
fcm45_Lb80	0.430	19.50	0.35	−0.45	2.75
fcm70_Lb40	0.189	21.50	0.24	−0.29	7.82
fcm70_Lb60	0.210	18.00	0.21	−0.29	3.37
fcm70_Lb80	0.345	18.20	0.19	−0.27	2.36
Average	0.250 (36.19%)	19.81 (6.60%)	0.21 (29.05%)	−0.32 (21.49%)	—

Note: Values in parentheses are coefficients of variation of corresponding series.

Notation

F_l = CFRP pullout force at loaded end;
$F_{l\,\max}$ = maximum CFRP pullout force;
f_{fu} = CFRP tensile strength;
s_f = free end slip;
s_l = loaded end slip;
$s_{l\,\max}$ = loaded end slip at maximum CFRP pullout force;
s_m = slip at peak bond stress;
t_f = CFRP thickness;
w_f = CFRP width;
α = parameter defining local bond stress-slip relationship;
α' = parameter defining local bond stress-slip relationship;
$\sigma_{l\,\max}$ = maximum CFRP stress;
τ = bond stress defining local bond stress-slip relationship;
τ_m = bond strength defining local bond stress-slip relationship; and
$\tau_{\max}$ = average bond strength at bonded length.

References

Alkhrdaji, T., Nanni, A., Chen, G., and Barker, M. (1999). "Upgrading the transportation infrastructure: Solid RC decks strengthened with FRP." *Concr. Int.*, 21(10), 37–41.

American Concrete Institute (ACI). (2002). "Guide for the design and construction of externally bonded FRP systems for strengthening concrete structures." *ACI Committee 440*, Farmington Hills, Mich.

Barros, J. A. O., and Dias, S. J. E. (2003). "Shear strengthening of reinforced concrete beams with laminate strips of CFRP." Proc., Int. Conf. of Composites in Construction, D. Bruno, G. Spadea, and N. Swamy, eds., Cosenza, Italy, 289–294.

Barros, J. A. O., and Figueiras, J. A. (1999). "Flexural behavior of SFRC: Testing and modeling." *J. Mater. Civ. Eng.*, 11(4), 331–339.

Barros, J. A. O., and Fortes, A. S. (2002). "Concrete beams reinforced

with carbon laminates bonded into slits." *Proc., 5th Congreso de Métodos Numéricos en Ingeniería* (CD-ROM), Madrid, Spain.

Blaschko, M., and Zilch, K. (1999). "Rehabilitation of concrete structures with CFRP strips glued into slits." Proc., 12th Int. Conf. of Composite Materials, Paris.

Comite europeo de normalizacion (CEN). (1987). "Métodos de ensaio de cimentos." *EN196-1* (European Norm), Bruxelles.

Concrete Society. (2000). "Design guidance for strengthening concrete structures using FRP composite materials." *Rep. No. 55*, Crowthorn, Berkshire, U.K.

Cosenza, E., Manfredi, G., and Realfonzo, R. (1997). "Behavior and modeling of bond of FRP rebars to concrete." *J. Compos. Constr.*, 1(2), 40–51.

De Lorenzis, L. (2002). "Strengthening of RC structures with near-surface mounted FRP rods." PhD thesis, University of Lecce, Italy.

De Lorenzis, L., Nanni, A., and La Tegola, A. (2000). "Flexural and shear strengthening of reinforced concrete structures with near surface mounted FRP rods." *Proc., 3th Int. Conf. on Advanced Composite Materials in Bridges and Structures*, J. Humar and A. G. Razaqpur, eds., Ottawa, 521–528.

De Lorenzis, L., Rizzo, A., and La Tegola, A. (2002). "A modified pull-out test for bond of near-surface mounted FRP rods in concrete." *Composites, Part B*, 33(8), 589–603.

Emmons, P., Thomas, J., and Sabnis, G. M. (2001). "New strengthening technology developed—Blue circle cement silo repair and upgrade." *Proc., Int. Workshop on Structural Composites for Infrastructure Applications*, T. Risk, ed., Cairo, Egypt, 97–107.

Ezeldin, A., and Balaguru, P. (1989). "Bond behavior of normal and high strength fiber reinforced concrete." *ACI Mater. J.*, 86, 515–524.

Ferreira, D. R. S. M. (2000). "Pilares de Betão Armado Reforçados com Laminados de Fibras de Carbono (Reinforced concrete columns strengthened with CFRP laminates)." MSc thesis, Civil Engineering Dept., University of Minho, Portugal (in Portuguese).

Focacci, F., Nanni, A., and Bakis, C. E. (2000). "Local bond-slip relationship for FRP reinforcement in concrete." *J. Compos. Constr.*, 4(1), 24–31.

German Institute of Construction Technology. (1997). "Strengthening of reinforced concrete and prestressed concrete with Sika Carbodur bonded carbon fiber plates." *Authorization No. 2-36.12-29*, Berlin.

Hogue, T., Cornforth, R. C., and Nanni, A. (1999). "Myriad convention center floor system reinforcement." *Proc., 4th Int. Symp. on Fiber Reinforced Polymer Reinforcement for Reinforced Concrete Structures*, C. W. Dolan, S. Rizkalla, and A. Nanni, eds., Baltimore, *ACI SP-188*, 1145–161.

International Federation for Structural Concrete (CEB-FIB). (2001). "Externally bonded FRP reinforcement for RC structures." *Rep. No. 14*, Task Group 9.3, FRP Reinforcement for Concrete Structures Lausanne, Switzerland.

International Organization for Standardization (ISO). (1997). "Plastics—Determination of tensile properties: Part 5. Test conditions for unidirectional fibre-reinforced plastic composites." *ISO 527-5*, Genève.

Larralde, J., and Silva-Rodriguez, R. (1993). "Bond and slip of FRP rebars in concrete." *J. Mater. Civ. Eng.*, 5(1), 30–40.

Malvar, L. (1995). "Tensile and bond properties of GFRP reinforcing bars." *ACI Mater. J.*, 92(3), 276–2985.

Mukhopadhyaya, P., and Swamy, N. (2001). "Interface shear stress: A new design criterion for plate debonding." *J. Compos. Constr.*, 5(1), 35–43.

Nguyen, D. M., Chan, T. K., and Cheong, H. K. (2001). "Brittle failure and bond development length of CFRP-concrete beams." *J. Compos. Constr.*, 5(1), 12–17.

Pantuso, A., Neubauer, U., and Rostasy, F. S. (2000). "Effects of thermal mismatch between FRP and concrete on bond." *4th ConFibreCrete Meeting*, Lille, France.

RILEM. (1982). "Bond test for reinforcement stell. 1: Beam test." *TC9-RC*.

Rossi, P. (1998). *Les bétons de fibres métalliques*, Presses de l'École National des Ponts et Chaussés, Paris (in French).

Rostasy, F. S. (1998). "Assessment of S&P CRP structural strengthening system." *Rep. No. 98/0322*, Scherer & Partners Construction System, Brunnen, Switzerland.

Sena-Cruz, J. M. S., and Barros, J. A. O. (2002a). "Bond behavior of carbon laminate strips into concrete by pullout-bending tests." *Proc., Int. Symp. on Bond in Concrete—From the Research to Standards*, G. Balazs, P. Bartos, J. Cairns, and A. Borosnyoi, eds., Budapest, Hungary, 614–621.

Sena-Cruz, J. M. S., and Barros, J. A. O. (2002b). "Caracterização experimental da ligação de laminados de CFRP inseridos no betão de recobrimento (Experimental characterization of CFRP laminates bonded to concrete cover)." *Rep. No. 02-DEC/E-15*, Dept. of Civil Engineering, Univ. of Minho (in Portuguese).

Sena-Cruz, J. M. S., and Barros, J. A. O. (2003). "Bond between near-surface mounted CFRP laminates and the concrete in structural strengthening." *Proc., Int. Conf. of Composites in Construction*, D. Bruno, G. Spadea, and N. Swamy, eds., Cosenza, Italy, 397–402.

Sena-Cruz, J. M. S., Barros, J. A. O., and Faria, R. M. C. M. (2001). "Assessing the embedded length of epoxy bonded carbon laminates by pull-out bending tests." *Proc., Int. Conf. on Composites in Construction*, J. Figueiras, L. Juvandes, and R. Faria, eds., Porto, Portugal, 217–222.

Toutanji, H., and Balaguru, P. (1998). "Durability characteristics of concrete columns wrapped with fiber tow sheets." *J. Mater. Civ. Eng.*, 10(1), 52–57.

Tumialan, G., Tinazzi, D., Myers, J., and Nanni, A. (1999). "Field evaluation of masonry walls strengthened with FRP composites at the Malcolm Bliss Hospital." *Rep. No. CIES 99-8*, Center for Infrastructure Engineering Studies, Univ. of Missouri-Rolla, Rolla, Mo.

Warren, G. E. (1998). "Waterfront repair and upgrade, Advanced Technology Demonstration Site No. 2: Pier 12, NAVSTA San Diego." *Rep. No. SSR-2419-SHR*, Naval Facilities Engineering Service Center, Port Hueneme, Calif.

Warren, G. E. (2000). "Waterfront repair and upgrade, Advanced Technology Demonstration Site No. 3: NAVSTA Bravo 25, Pearl Harbour." *Rep. No. SSR-2567-SHR*, Naval Facilities Engineering Service Center, Port Hueneme, Calif.